UC-94e
LBL-17971
Preprint c.1

Lawrence Berkeley Laboratory
UNIVERSITY OF CALIFORNIA

Materials & Molecular Research Division

RECEIVED
LAWRENCE
BERKELEY LABORATORY
OCT 9 1984
LIBRARY AND
DOCUMENTS SECTION

Submitted to Surface Science

AES AND TDS STUDIES OF ELECTROCHEMICALLY OXIDIZED Pt(100)

F.T. Wagner and P.N. Ross, Jr.

July 1984

For Reference

Not to be taken from this room

LBL-17971 c.1

Prepared for the U.S. Department of Energy under Contract DE-AC03-76SF00098

DISCLAIMER

This document was prepared as an account of work sponsored by the United States Government. While this document is believed to contain correct information, neither the United States Government nor any agency thereof, nor the Regents of the University of California, nor any of their employees, makes any warranty, express or implied, or assumes any legal responsibility for the accuracy, completeness, or usefulness of any information, apparatus, product, or process disclosed, or represents that its use would not infringe privately owned rights. Reference herein to any specific commercial product, process, or service by its trade name, trademark, manufacturer, or otherwise, does not necessarily constitute or imply its endorsement, recommendation, or favoring by the United States Government or any agency thereof, or the Regents of the University of California. The views and opinions of authors expressed herein do not necessarily state or reflect those of the United States Government or any agency thereof or the Regents of the University of California.

LBL-17971

AES AND TDS STUDIES OF ELECTROCHEMICALLY OXIDIZED Pt(100)

F.T. Wagner and P.N. Ross, Jr.

Materials and Molecular Research Division
Lawrence Berkeley Laboratory
University of California
Berkeley, CA 94720

This work was supported by the Assistant Secretary for Conservation and Renewable Energy, Office of Advanced conservation Technology, Division of Electrochemical Systems Resources of the U.S. Department of Energy under Contract Number DE-AC03-76SF00098.

AES AND TDS STUDIES OF ELECTROCHEMICALLY OXIDIZED Pt(100)

F.T. Wagner* and P.N. Ross, Jr.

Materials and Molecular Research Division
Lawrence Berkeley Laboratory
University of California
Berkeley, CA 94720

Abstract

Anodic films formed on Pt(100) in 0.3M HF using a quasi thin-layer electrochemical cell within a vacuum envelope were transferred to ultra-high vacuum for study by AES and TDS. Films generated at potentials above 1.1V survived emersion and pumpdown in a hydrated state. As the emersion potential increased, the integrated H_2O and O_2 thermal desorption signals increased in parallel, indicating a contant stoichiometry consistent with the presence of a platinum hydroxide layer. The oxygen TDS and AES signals after holding the electrode at constant potential for several minutes saturated above 1.9V(RHE) with formation of a surface phase containing 2.3 O/Pt (desorbing as O_2), but much thicker films could be grown by AC polarization. For all films water desorbed at temperatures well below those for oxygen evolution. ESCA and TDS showed the composition of the thick films to be $Pt(OH)_4$. O_2 thermal desorption from thin films gave a shift from 570 to 630K in the desorption maximum as the initial coverage increased. Three desorption models were compared with the experimental data: desorption at the perimeters between covered and uncovered patches, autocatalytic desorption, and first-order desorption with variable activation energy. Perimeter-controlled desorption gave the best overall fit with data, indicating a growth mode for aged anodic films involving island growth and fusion.

Qualitative similarities with previously-reported TDS data for high coverage states of gas-phase adsorbed oxygen suggests that desorption may occur predominantly at the edges of saturated patches in both cases, while chemical differences between place-exchanged anodic oxygen and surface adsorbed oxygen account for lower desorption temperatures and higher saturation coverages for the former. Water evolved from both thick and thin anodic films at 400K, a temperature much higher than that reported for surface adsorbed hydroxyl groups produced by low-temperature gas-phase coadsorption of O_2 and H_2O [1]. The higher temperature desorption is ascribed to the incorporation of hydroxyls in a surface phase involving place exchange between Pt and O atoms.

---

* Present address: Physical Chemistry Department, General Motors Research Laboratories, Warren, MI 48063

1. Introduction

The electrochemical interactions of oxygen and water with platinum are central to the operation of metal-air batteries, fuel cells, and electrolyzers, in which Pt-group metals or their alloys have proven to be the best electrocatalysts. Anodic oxides on platinum have been studied extensively by electrochemical and optical techniques and to a lesser extent by UHV surface analytical methods, but the composition and hydration of the films remain subjects of controversy. Much discussion has centered upon the distinction between adsorbed oxygen and phase oxides, the latter being defined as involving disruption of the Pt metal lattice [2]. Biegler and Woods [3] explained electrochemical stripping data with an adsorbed oxygen state which reached a limiting coverage of 2.66 O/Pt at 2.2V(RHE). Thacker and Hoare [4], also using stripping studies, concluded that, after surface adsorption started at 0.8V, dermasorption (sorption into the first few layers of the metal) commenced at 1.0V. Dermasorption and surface adsorption continued together up to 1.6V, where a monolayer of PtO was thought to be present. At higher potentials some of the PtO was further oxidized. Vetter and Schultze [5], also analyzed charging and stripping curves and concluded that the coverage of adsorbed oxygen did not exceed a few percent, with a rate-determining, field-dependent place exchange leading to a phase oxide that represented most of the anodic charge. Fleischmann et al. [6] proposed the formation of four different "oxides" on Pt anodes. Angerstein-Kozlowska et al. [7] have given the most detailed interpretation of voltammetric and ellipsometric data to date. They have proposed a series of oxidation steps which occur as a polycrystalline Pt electrode is swept to

progressively higher potentials in acidic electrolyte. The initial oxidation, in the potential region 0.8-0.93V(RHE), was ascribed to reversible hydroxylation of the surface. Above 0.93V place exchange between adsorbed hydroxyl species and Pt occurs, and electrochemical irreversibility sets in. The place exchange is a rather slow process, and leads to complex aging behavior. In the potential range of ca. 1.0 to 1.2V (depending upon time factors) the peak potential of the subsequent reduction wave is independent of the total oxidation charge. This invariance was ascribed to constant Pt-O geometry, and the charge passed in this region was considered due to oxidative deprotonation of the hydroxyls previously incorporated into the surface. The above conclusions were based upon analysis of details of cyclic voltammetry curves. Optical studies showed that for oxidation up to a charge of $0.6e^-/Pt$ the same value of the ellipsometric parameter Δ was observed for a given surface charge on both the anodic-going and cathodic-going sweeps. For more complex oxidations the Δ/Q curves for the anodic and cathodic sweeps diverged, suggesting that the oxidized species first formed was also the first reduced. This species was suggested to be the reversible hydroxyl groups residing at the surface. A change in the Δ/Q slope at $0.5e^-/Pt$ (anodic direction) was ascribed to the onset of formation of the deprotonated oxide. At 1.0 e^-/Pt (1.13V) a further change was seen in the Δ/Q slope, which then continued unchanged out to at least 2 e^-/Pt. The identification of the individual chemical species in this complex scheme was indirect and has awaited confirmation by direct spectroscopic and structural studies.

Attempts to identify the anodically formed surface species on Pt electrodes directly by spectroscopy have met with little success. Ellip-

sometry has been used in a number of studies [8-12] and while changes in the optical properties of the anodic film were observed at certain potentials and/or coverage, the interpretation of these changes was problematic, and the results were limited to estimation of layer thicknesses of "oxides" of indeterminate chemistry. Ex-situ analysis of anodic layers by XPS has been used in attempts to identify the oxidation state of Pt surface atoms. Hammond and Winograd [13] used glove-box transfer and ESCA to characterize Pt foils oxidized potentiostatically at 1.92-2.54V (RHE). Their deconvolution of the data for the limiting oxide yielded a Pt 4f 7/2 line at 73.6eV (shifted 2.6eV from metallic Pt), ascribed to Pt in the (+II) state based upon a reference PtO material whose composition is controversial [14,15]. After anodization at 2.54V they reported indications of an additional peak at 74.4eV ascribed to Pt (+IV). Brandt [16] found the predominant oxidized Pt 4f 7/2 line for foils anodized at 1.25-3.25V (RHE) to lie at 73.8eV, a binding energy which did not allow certain discrimination between Pt (+II) and Pt (+IV). Long polarization at 3.25V led to a major peak at 74.1eV.

The interactions of gas-phase water and oxygen with single-crystal Pt surfaces have been extensively studied under UHV conditions, but the extent to which conclusions drawn from such studies are applicable to electrochemical conditions have not been adequately tested. Fisher and Gland [18] reported that sub-monolayer quantities of water adsorbed on Pt (111) at low temperature desorbed completely around 180K with a reaction order suggestive of a rate-limiting step at the edges of water patches. Vibrational spectroscopy of this system also showed that hydrogen bonding and clustering occurred even at submonolayer coverages [19]. Ibach and Lehwald [20] observed similar clustering and desorption at 170K on Pt (100). In the

presence of oxygen preadsorbed on Pt (111), water adsorption led to the formation of surface hydroxyl groups [1]. Water desorbed upon heating the hydroxylated surface to 215K. A number of studies [21-23] have shown that anhydrous oxygen adsorbs dissociatively on Pt (111) at room temperature to give an ordered 2x2 structure, saturating at 0.25 oxygen atoms per surface Pt atom, which desorbs at 700-850K. On Pt(100) substantial adsorption of oxygen requires dosing at elevated temperatures. Barteau et al. [24] and Derry and Ross [23] both reported unusually sharp desorption features around 660K. The latter work, using variable take-off angle XPS, showed that the oxygen in the high coverage state (O/Pt=0.75-1.0) resided on, not under, the surface. Little if any chemical shift from the metal was observed in the Pt 4f lines. However, formation in UHV of phase oxides of Pt from which oxygen desorbs at 1200K or higher has been reported by a number of groups [25-27]. In at least some cases these oxides have been related to the presence of impurities such as Si and Ca [28], but controversy remains on this subject [25].

The present work was undertaken to provide a bridge between the electrochemical and UHV studies of water and oxygen on Pt. Electrochemically grown films were cleanly transferred to vacuum and subjected to the same analytical techniques as were used in the cited low-pressure UHV studies of oxygen and water adsorption on Pt . This paper deals with the determination of the composition of anodic films by AES and TDS analysis. The atomic-scale structural consequences of anodic film formation as determined by LEED are the topic of a second paper [29]. The results show some parallels between the surfaces formed electrochemically and the surfaces

formed by low-pressure interaction with gases, but sufficient differences were also observed that suggest the need for caution in the use of conclusions drawn from low-pressure UHV experiments in developing a picture of the solid-liquid interface.

2. Experimental

The directly coupled electrochemical-UHV surface analysis system used in these studies has been described in detail elsewhere [30,31]. Clean, ordered, well-characterized Pt (100) surfaces prepared by standard UHV techniques were moved to a turbomolecularly-pumped transfer chamber by means of a long-throw magnetically coupled manipulator. This chamber was then backfilled to near atmospheric pressure with electronic-grade argon further purified by passage through high purity Ti sponge at 1200K. This improved treatment of the backfill gas has led to a 3 to 4-fold reduction in the carbon contamination of the surface reported previously [30], leaving the Auger equivalent of 0.1 graphite layers on the surface after exposure to backfill gases plus electrolyte vapor and pumpdown as shown in Fig. 1. No additional contamination as seen by Auger was picked up upon contact with the liquid electrolyte itself. An electrochemical cell, featuring an α-Pd hydride reference electrode and a Pt ring counterelectrode to which a ca. 100μl droplet of 0.3M HF had been previously admitted, was lowered to make contact with the crystal under potentiostatic control. The electrolyte was prepared from Ultrex-grade 40% HF and Harleco ultra-pure water and was further purified by Pt pre-electrolysis in the external reservoir. In most

of the experiments reported here the crystal was held at a given potential for about 2 minutes, after which time the transfer chamber was slightly overpressurized with Ar to drive the electrolyte cleanly out from the gap between the crystal and the counter-reference electrode assembly into a capillary leading to an external electrolyte reservoir. This emersion technique leaves an electrolyte film ca. 4000Å thick adhering to the crystal face [32]. The electrochemical cell was then pulled up and valved off, the transfer chamber was evacuated, and the crystal was returned to UHV for post-electrochemical analysis.

AES was performed with a single-pass cylindrical mirror analyzer equipped with an on-axis electron gun. The electron beam could be rastered and an image obtained in either the absorbed current or the secondary emission mode. This imaging capability allowed determination of the fraction of the crystal surface which had been in contact with the electrolyte, allowing normalization of coulometry and thermal desorption intensities to the actual anodized area.

Thermal desorption data were obtained with a Spectramass 1000M residual gas analyzer controlled by an LSI-11/23-based minicomputer to allow several mass peaks to be monitored. The ionizer of the gas analyzer was mounted within a conical Ta nozzle tube [33] with a 6.4 mm aperture next to which the crystal face could be placed. The nozzle increased the signal due to molecules desorbing from the crystal face while discriminating against molecules from the support structures. Identical oxygen desorption peak shapes were obtained with and without the nozzle in place, indicating that in both cases the effective pumping speed was sufficiently rapid to keep the

signal proportional to the desorption rate. The crystal was gold-brazed to a Ta cup, which was held in a stainless-steel transfer frame. This frame positioned the cup in front on the Ta filament used for radiant heating of the sample. Time-temperature curves for a give heating current were obtained with a Pt-Pt/10% Rn thermocouple spot-welded to the crystal and used to calibarate an infrared pyrometer. Use of the pyrometer allowed confirmation of the reproducibility of the time-temperature function when the thermocouple was removed to permit the crystal to be transferred to the electrochemical cell. A heating rate of 11 Ks^{-1} was used in all experiments unless otherwise noted.

Thermal desorption data were quantified by comparison of integrated TDS signals with those obtained from the saturation coverage of CO on Pt(100). The latter coverage has been calibrated at 0.77 CO/surface Pt by Davies and Norton [34] using nuclear reaction methods. The sensitivity of the gas analyzer to CO, O_2, and H_2O was experimentally determined for comparable ion-gauge pressures of the pure gases, and published sensitivity factors for the ion gauge [35] were then mixed in to give correct relative sensitivity factors for the RGA.

3. Results

In this work three techniques, Auger electron spectroscopy, thermal desorption spectroscopy, and coulometry, were used to study the composition of thin anodic films. These methods differ in their sensitivity to the oxidation and hydration of the surfaces; some consideration should be given

to these differences so that the detailed results below can be understood in their proper contexts.

Coulometry is the classical electrochemical technique whereby the extent of anodic film growth has been followed. The reference oxidation states for the anodic film-free Pt surfaces in these studies are Pt(0) in metallic Pt, O(-II) in H_2O, OH^-, and H_3O^+, and F(-I) in F^-. For Pt(100) 1x1 the passage of 209$\mu C/cm^2$ of anodic charge corresponds to $1e^-$ oxidation per surface Pt atom. While coulometry provides a sensitive in-situ measure of the oxidation state of a surface, it gives no indication of the hydration state since the water of hydration remains in the reference oxidation state.

Thermal desorption spectroscopy measures both the oxidation and hydration states of anodic films on Pt after their emersion and evacuation. Upon heating, the anodic films evolved molecular H_2O and molecular O_2. Since water is in the reference oxidation state, its desorption constituted a dehydration, but not a reduction, of the films. On the other hand, each O atom desorbing as O_2 represented a $2e^-$ oxidation from the reference O(-II) state during film formation. Since no desorption of other oxidized species such as O_2, $OH\cdot$, $F\cdot$, or F_2 was observed, and since heating the films to 820K completely reduced them to metallic Pt, the integrated O_2 thermal desorption measured the total level of oxidation of the emersed and evacuated films.

The O/Pt Auger peak ratio, in the absence of beam effects, should measure all oxygen atoms on the surface, both those destined to desorb as O_2 and those desorbing in H_2O. However, the Auger beam rapidly dehydrated the surface, as will be shown in section 3.3. The Auger-determined oxygen

thus corresponded to an oxidation above the reference state of about $2e^-$ per O atom, rather than to the combined hydration and oxidation.

3.1. Anodic film composition as a function of potential

Anodization of UHV-prepared Pt(100) for ca. 2 min. at potentials above 1.1V(RHE)[†] produced films which survived emersion and evacuation with at least some of the hydration water intact. Figures 2, 3, and 4 show the O/Pt Auger signal ratio, the integrated O_2 thermal desorption signal (M/e=32), and the integrated H_2O thermal desorption signal (M/e=18) as functions of emersion potential. All three signals showed a similar increase in intensity with increasing potential over the region 1.1-1.9V. The parallel increases in the oxygen and water desorption signals indicate the growth of a hydrated film of nearly constant stoichiometry (approximately $PtO_x \cdot xH_2O$) rather than the growth of an anhydrous oxide under a constant hydration sheathe as suggested by the tritium data of Schultze [17]. Above 1.9V the leveling out of the Auger and O_2 thermal desorption signals indicate the formation of a passive layer which prevents further oxidation on the ca. 2 min. time scale of these experiments. According to thermal desorption data the saturated passive film contained 2.3 O atoms (desorbing as O_2) and 2 water molecules per surface Pt atom on the 1x1 Pt(100) surface. Stripping coulometry following transfer to UHV and return gave good agreement with the O_2 TDS measurements, yielding 1040μC/cm^2 (equivalent to 2.5 O atoms/surface

---

[†]All potentials given in this paper are referenced to the reversible hydrogen electrode in the same electrolyte (RHE).

Pt atom) for a film formed at 2.2V. This level of agreement indicates the validity of the calibration of the thermal desorption data based on the saturated layer of adsorbed CO.

3.2 Structure of anodic films

Low energy electron diffraction from anodic films formed above 1.5V on well-ordered Pt(100) or (111) surfaces gave only a general diffuse background with no defined spots, indicating the lack of order in the films. LEED patterns for films formed at lower potentials showed only diffuse background and partially attenuated substrate spots. The films remained disordered after being dehydrated by heating to 450K. Electrochemical reduction of the anodic films removed the oxygen and restored the substrate LEED spots. Repetitive oxidation/reduction cycling produced LEED patterns with spot sizes modulated by changes in the beam energy in a manner suggestive of the introduction of predominantly monatomic steps [30]. Since thermal reduction of the film required temperatures sufficiently high to anneal out most of the electrochemically induced defects, direct comparison of the atomic-scale structural effects of thermal and electrochemical reduction is impossible. Detailed description and analysis of the structural changes induced by repeated redox cycling are given in another paper [29]. Here it is sufficient to note that formation and reduction of the thin films discussed in this paper left the local order of the surface largely intact through quasiepitaxial reduction of the amorphous films, but the introduction of steps indicates that place exchange of Pt and O atoms during anodization at 100mV/s starts at 1.0V and becomes more pronounced above 1.2V.

The general properties of the anodic films have been outlined in the preceeding two sections. Each of the techniques used in these studies has a subtly different response to nonidealities inherent in surface science experiments performed on surfaces prepared in a medium 10^{15}-fold more dense than the UHV environment. These nonidealities include such effects as vacuum dehydration, gas-phase cleanoff reactions, electrochemical self-discharge, and electron beam damage. The results of each technique will now be considered in detail.

3.3. Auger electron spectroscopy

The AES O(513eV)/Pt(238eV) peak ratio increased with anodization potential as shown in Fig. 2. The ratios in Figure 2 are steady-state values obtained with a static electron beam focused to ca. 100μm. Under these conditions no significant changes in the peak ratio were seen for beam exposure times of 5s to 1 hr. A representative Auger spectrum for Pt(100) emersed at 1.9V is given in Figure 5. The O(513eV)/Pt(238eV) peak ratio of 4.6 is about ten-fold larger than the maximum value reported for low-index Pt dosed with oxygen from the gas phase (22). The O KVV/KLV peak ratio of 2.5 is smaller than that for most oxides but is similar to that previously reported for O adsorbed on Pt (36). N(E) spectra obtained by beam-blanking showed that this low N'(E) peak ratio was due to an unusually broad KVV peak. When the electron beam was rastered over the maximum area consistent with good spectrum resolution (ca. 3x3mm), larger O signals with more typical oxide peak shapes were observed for the first few tens of seconds of

beam exposure. Rastering the beam for extended times over most of the electrolyte contact area significantly decreased the water thermal desorption signal, as shown by the point marked by the triangle in figure 4. The initial rapid decrease in the oxygen Auger signal thus corresponded to a beam-induced dehydration of the surface; once dehydrated the surface was stable to the beam. The steady-state Auger signal obtained with the static electron beam arose from the anhydrous oxide produced locally from the original hydrous film. Since the Auger analysis area was much smaller than both the electrolyte contact area and the aperture of the gas analyzer nozzle, normal Auger analysis had no significant effect on the results of susequent thermal desorption experiments. Under conditions of maximum beam raster (ca. 15x15mm) at low beam energies, beam damage was sufficiently slow that an adsorbed current image could be taken to identify the electrolyte contact area without significantly dehydrating the surface.

Auger analysis with both static and rastered beams showed no incorporation of the fluoride anions from the 0.3M HF electrolyte into the anodic films. In the same apparatus fluoride was readily detected in anodic films formed in 0.3M HF on Ta, a material for which anion incorporation has been previously demonstrated by other means [37]. Although no traces of the major anion, fluoride, were found in the anodic films, small levels of chlorine, a common impurity in HF as chloride, were seen by Auger. This observation is in concert with electrochemical results which have indicated that Cl^- interacts much more strongly with Pt than does F^- [38]. Over the emersion potential range of 0.0-1.1V the Cl Auger signal was almost constant, corresponding to a Cl/Pt surface atomic ratio of 0.01 (based upon a monolayer HCl on Pt Auger spectrum published by Garwood and Hubbard [39]). In

anodic films a larger chlorine signal was seen which decreased at higher potentials from a surface atomic ratio of ca. 0.08 at 1.2V to ca. 0.02 at 1.95V.

As monitored by oxygen AES, the hydrated anodic films were stable to UHV conditions. Overnight exposure to background gases (10^{-10} torr range) caused no significant diminution of the oxygen Auger signal. However, the oxygen signal from a film dehydrated by partial thermal desorption disappeared after extended exposure to background gases. The oxygen signal for a hydrous film was completely removed by brief exposure to 1 torr H_2. This reactivity, plus the lack of Auger signals at 296eV (Ca), and 1606eV (SiO_2) show that the observed oxygen signals were not due to the oxidation of impurities often found in Pt crystals as may have been the case for some "Pt oxides" grown from the gas phase [28].

3.4. TDS of thin anodic films

Upon heating, anodic films formed in 0.3M HF evolved H_2O and O_2 at widely separated temperatures (Fig. 6). Interruption of the thermal ramp after the water peak appeared had no effect on the temperature, shape, or size of the subsequent O_2 desorption peak, showing that dehydration and thermal reduction were separate processes. The integrated O_2 and H_2O TDS signals increased in parallel, indicating a constant film stoichiometry of $PtO_x \cdot xH_2O$. At the highest O/Pt ratios observed, a small evolution of oxygen accompanied the start of dehydration, but this never amounted to a large proportion of the total oxygen desorbed from the anodic films.

3.4.1. Water thermal desorption

Water was evolved in a single broad peak at 400K, a much higher temperature than the 170K reported for low-pressure, low-temperature dosed clean Pt (100) [19] or the 215K reported for low pressure, low temperature water co-adsorption with oxygen on Pt (111) [1]. The peak temperature and shape were invariant with coverage as would be expected for a dehydration process first-order in the water-containing species. Application of the Redhead correlation of peak temperature with activation energy (assuming a pre-exponential of $10^{13}s^{-1}$) [40] yielded an activation energy of 24 kcal/mole, twice the heat of sublimation of water. Since the peak shape showed asymmetry opposite to that expected for a simple first-order process, it is unlikely that this simple model accurately describes the desorption process. However, even without an accurate model, the high desorption temperature shows a stronger binding of water on the electrochemically anodized surfaces than has been seen in gas-phase water dosing experiments on either clean or oxygen pre-dosed surfaces.

Some water desorbed at 400K from surfaces emersed at all potentials, including potentials below the point of zero charge. Less than 0.5 water molecules per surface Pt atom desorbed from surfaces which showed no Auger or TDS oxygen. Once water was removed by partial desorption (to ca. 450K), it could not be replaced on the room temperature crystal by a 100L dose of water vapor at 10^{-7} torr, showing that this water was not bound to trace alkali impurities from the electrolyte. Such impurities could at times be detected at the spot where the capillary which removed the electrolyte from

the cell had touched the crystal. These small patches of alkali oxides/ hydroxides remained on the surface after partial desorption experiments; had they or other thermally resistant impurities (such as the small amounts of C,S, and sometimes Cl picked up during transfer) contributed significantly to the initial water desorption signal a similar signal should have been seen after dosing with water vapor. Comparison of experiments run with and without the nozzle tube around the ionizer of the gas analyzer showed that, while the broad water desorption background seen in Figure 6 did arise from support structures, the peak at 400K evolved from the crystal face. Measurable CO_2 (M/e=44) desorbed from the crystal face in the same temperature range as water. Avery [41] has reported CO_2 evolution from decomposition of carboxylate species at similar temperatures on Pt (111) and it seems most likely that the water observed desorbing from nonoxidized Pt electrodes (i.e. potentials below 1.2V) was associated with carboxylic impurities. However, at emersion potentials above 1.2V the water and oxygen thermal desorption signals both increased with increasing potential, maintaining a roughly constant ratio of one water molecule desorbed per oxygen atom desorbing as O_2. The increase in water desorption signal with increasing oxidation of the surface was too large to be accounted for by impurities; it corresponded to the presence of a hydrated phase oxide or hydroxide.

3.4.2. Oxygen thermal desorption.

O_2 (M/e=32) desorbed from Pt(100) anodized in acidic electrolytes in a sharp primary peak at 570-630 K with smaller features at higher temperatures. The same complex structure was seen in O_2 desorption from two

different Pt(100) crystals anodized in HF and also from Pt(100) anodized at 1.58V in $5x10^{-3}$M H_2SO_4. As shown in Fig. 7, the temperature at which the maximum desorption rate occurred, T_p, increased with increasing coverage. The leading edges of the desorption curves for different coverages did not align as would be expected for a simple zeroth-order process governed by a constant activation energy [42]. Rather, the leading edges and peaks for lower coverages occurred at lower temperatures than were observed for the same desorption rates from more heavily oxidized surfaces. The shift in T_p showed a continuity of behavior over an emersion potential region of at least 1.35-2.1V(RHE). The O_2 desorption curves from Pt(100) displayed a shoulder at ca. 640K which showed a lesser snift in temperature for different coverages. At the limiting coverage the low temperature main peak overlapped this higher temperature shoulder. At the lowest transferable coverages only the 'shoulder' was seen. The main peak and shoulder could not be separated by interruption of the heating ramp; i.e. once desorption started it continued until all of the oxygen in both the main peak and the shoulder had left the surface.

At 725 K another small peak was seen which became larger but shifted slightly, if at all, to higher temperature at higher coverages, suggesting a zero to first-order desorption process. This peak could be at least partially isolated by stopping heating at 650 K. When the crystal was then cooled and reheated, the remaining oxygen desorbed at 725 K, showing that the oxygen in this peak is kinetically distinct from that in the lower temperature features. The area under this peak was a relatively constant 10-15% of the total O_2 desorption area. As will be seen in section 3.5,

this peak was similar in temperature to that observed for a thick anodic film, suggesting that the peak corresponds to islands of thicker film on the otherwise uniform anodic layer. The fact that the anodic film saturated at O/Pt=2.3 rather than 2 (by TDS) also suggests ca. 15% of the anodic charge going into thicker islands while the rest of the surface is passivated by a uniform "monolayer" of anodic film. This "monolayer" is actually several atomic layers thick when oxygen, hydrogen, and displaced Pt atoms are taken into account.

The inability to separate the 640K shoulder from the main thermal desorption peak by interruption of the heating ramp suggests that this shoulder, unlike the 725K peak, is kinetically associated with the main peak at 570-630K. Even without the added complication of this shoulder, the behavior of the main TDS peak suggests a complex desorption mechanism. Considering first simple n-th order desorption with constant activation energy, the increase in T_p with coverage suggests that $n<1$. The leading edges of the lower coverage peaks lie outside those for higher coverages, contrary to the expectations for 1/2 or 0 order for which the low coverage leading edges should lie, respectively, inside or on top of the high coverage leading edges. The data thus indicate a process with a negative reaction order in surface coverage. Three different models capable of producing such negative reaction order for the desorption rate were developed and compared to the experimental results: a perimeter-controlled desorption model, and two different autocatalytic models. As shown by Fig. 8, all three models could produce a sharp peak which shifts to higher temperature at higher coverage with activation energies around 20 kcal/mol O_2. However, only the

perimeter-controlled desorption model had the double peak structure at intermediate coverages, with the sharp low-temperature peak growing with coverage to become the predominant peak, as observed by TDS. This model also avoided the problems with low pre-exponential factors and assumption of surface mobility for oxygen in a surface phase oxide which beset the other two models. Since the perimeter-controlled desorption model has important implications for the mechanism of thermal reduction of anodic films, and possibly for the growth mechanism as well, we shall describe this model here in some detail. The details of the other two less satisfactory models are described in the Appendix.

In the perimeter-controlled desorption model, the rate of desorption is assumed proportional to the total perimeter length between covered and uncovered sections of the surface. For desorption from high initial coverages the perimeter length first increases, then decreases, as the open patches grow and then fuse. For full initial coverage the model assumes nucleation of open patches at spots defined by a square mesh. As desorption proceeds the open patches grow as expanding circles with constantly increasing perimeter until they grow tangent to one another. With further desorption the perimeter decreases as the circular arcs continue to advance from their original centers; at this point the covered patches resemble squares with slightly concave sides. Subunity initial coverages are assumed to have the geometry which would result from desorption of a saturated surface down to the given coverage. This assumption corresponds to a mode of film growth in which isolated patches of the film grow up to the point of tangency,

after which they fuse and the open holes are filled in. The exact geometric form of the model is an idealization, but it does provide the simplest perimeter-controlled model which can take into account both the growth and fusion of patches. Assumption of different geometries or a mix of patch sizes would serve primarily to shift the coverage at which the tangency point is reached.

The curves in Fig. 8a were produced by numerical integration of the equation

$$-d\theta/dt=p(\theta).(\nu/d).\exp(-E_a/RT)$$

where ν is the preexponential, d is the spacing of the patch grid, E_a a constant activation energy, and $p(\theta)$ the perimeter around a given grid point at coverage θ. Since for coverages below the tangency point ($\theta<1-\pi/4$) the perimeter could not be expressed as an explicit function of θ, the curves were generated using a table lookup program for the explicit function of θ in the patch radius over this coverage range. The shape of the curves was independent of details of the partitioning for numerical integration around the tangency point.

At the lowest coverages this model gave a single peak with a broad leading edge similar to that observed for the anodic film formed at 1.3V (Fig. 7). For coverages just above the tangency point a sharp peak arose on the leading edge of the broader peak, mimicking experimental behavior. With further increases in initial coverage the sharp peak shifted to higher temperatures while the broad peak showed a lesser shift. The activation energy

and the ν/d ratio were juggled to give best agreement of the main peak temperatures with experimental data over the entire experimental coverage range. The best fit was obtained with $E_a = 21 \pm 5$ kcal/mol and $\nu/d = 10^{13}-10^{15}$ $cm^{-1}s^{-1}$. This model reproduced the observed behavior of the broad peak at low coverage and the sharp peak which grew in at lower temperature, then moved up to higher temperatures at higher coverages. The separation between broad and sharp peaks in the model was not as great as that observed experimentally, possibly due to the assumption of uniform patch sizes in the model. The reasonable general agreement between model and experiment suggests both a perimeter-controlled mechanism of desorption and growth of the film through island expansion and fusion. In this model the fusion of islands during growth leaves uncovered holes whose perimeters increase during the initial stages of desorption. Previous perimeter-controlled desorption models [43] leading to simple 1/2-order kinetics have implicitly postulated island growth without fusion at higher coverages; no enclosed uncovered holes were formed and the total perimeter length continuously decreased during desorption. In the case of the ordered films observed in those studies, repulsions between antiphase domains might prevent island fusion. Since the anodic films discussed here show no order by LEED, no such specific repulsions would be present. The dielectric medium present during anodic film growth could also screen repulsions between islands, allowing fusion at boundaries without changes in the overall shape of the islands.

3.5. Thick anodic films

Although the formation of a thin passivating anodic film on Pt has been indicated by the present Auger and thermal desorption work on single crystals and by some previous electrochemical work on foils [2,3,44], other investigators have reported the formation of thick (on the order of at least 10^{-7}m) films during prolonged direct-current anodization [45]. At least in some cases the thick film formation was enhanced by mechanical introduction of defects [46]. Burke et al. [47] have employed a technique of rapid potentiodynamic cycling between the double-layer and oxide regions which reliably produces thick anodic films on Pt without recourse to mechanical roughening. Figure 9 shows thermal decomposition results for a polycrystalline foil oxidized in 0.3M HF by cycling at 0.3Hz between 0.5 and 2.4V for ten minutes. This treatment produced a compact-appearing layer with a gold interference color which graded to purple and blue around the edges. The appearance of the film was unaltered by drying and evacuation. As in the case of the thin films, water came off upon heating in a single broad peak at 400K (Fig.9). The major O_2 evolution occurred in a single peak at 715K, with minor oxygen loss accompanying dehydration. No higher temperature structure was seen in the O_2 TDS. One water molecule was evolved for every oxygen atom which came off as O_2. The thick film was quite stable to exposure to ambient atmosphere, allowing anodized foils to be carried through the air and mounted in a second vacuum system equipped with a double-pass cylindrical mirror analyzer and X-ray source for ESCA analysis. This technique yielded a broad Pt 4f 7/2 line at 74.2eV indicative of Pt in

the (+IV) oxidation state. This result, combined with the 2:1 $H_2O:O_2$ ratio from TDS, identifies the stoichiometry of the thick film as $PtO_2 \cdot 2H_2O$. A single broad oxygen 1s line was seen at 530.7eV binding energy. Fisher and Sexton [1] have reported that oxygen and water adsorbed separately from the gas phase yielded O 1s peaks at 529.8 and 532.3eV, respectively. They assigned a peak near 531eV to a surface-bound hydroxyl group formed after adsorption of both oxygen and water. On the basis of this assignment the thick anodic film on Pt appears to be best described as $Pt(OH)_4$. Since heating to 500K caused dehydration without reduction (presumably to PtO_2), the O_2 peak at 730K is characteristic of the bulk anhydrous oxide and provides a point of comparison in the controversy over the nature of high-temperature stable oxygen on Pt single crystals [25,28].

Auger analysis of the thick film gave a static-beam O(513eV)/Pt(238eV) peak ratio of 9.3 with an oxygen KVV/KVL ratio of 2.56 indicative of the same unusual peak shape seen for adsorbed oxygen and for the thin films. The time evolution of the oxygen signal again suggested the rapid beam-induced dehydration of the entire region sampled by Auger. As in the case of the thin films, Auger showed no indication of the incorporation of the fluoride anion in the thick anodic film. No chlorine was detected, nor were Si,Ca, or Na found present except for significant SiO_2 found on one film grown using 0.3M HF in a glass electrochemical cell instead of in the normal polytetrafluoroethylene cell.

4. Discussion

4.1 Composition of thin films 0.8-1.1V(RHE)

Films formed in the potential region 0.8-1.1V did not survive emersion and transfer and were visible only in cyclic voltammetry. The upper limit corresponds to the potential at which LEED showed that restructuring of the surface by a few oxidation cycles became substantial [29,31], though slight restructuring started at 1.0V. Such restructuring indicates the formation of a surface phase oxide which involves the motion of Pt atoms out of their metallic lattice positions. The absence of restructuring at the lower potentials suggests that under these conditions the film is best described as a surface-adsorbed OH or O species. The low-potential films are at least somewhat analogous to the adsorbed oxygen and hydroxide species studied in UHV using gas-phase dosing, which show marked reactivity towards reducing species such as CO and H_2O. The surface oxygen formed in this potential range is lost either through gas-phase reactions similar to the CO cleanoff observed in UHV with reducing impurities in the backfill gases or by reduction coupled to oxidation of species in the thin layer of electrolyte which adheres to the surface during emersion. Either impurities or possibly hydrogen introduced to the electrolyte from the palladium hydride reference electrode could provide the reductive capacity necessary to account for the loss of the surface oxygen layer. As discussed by Angerstein-Kozlowska et al. [7] anodic films formed at the lowest potentials are electrochemically reversible; i.e. any decrease in electrode potential causes a decrease in

coverage. The presence of any species which can react to lower the potential once the electronic continuity of the three elctrode cell is broken thus can cause the disappearance of the surface adsorbed oxygen. Above 1.2V extensive Pt-O place exchange decreases the electrochemical reversibility of the films, which then survive emersion and evacuation.

4.2. Composition of thin films 1.1-2.2V(RHE)

Over the transition region of 1.1-1.4V an increasing proportion of the anodic film survived emersion and transfer. In this potential interval LEED showed that the extent of restructuring of the surface per oxidation/reduction cycle also increased with potential, suggesting that a higher percentage of the surface Pt atoms undergo place exchange as the potential is increased over this interval. Angerstein-Kozlowska et al. [7] have given a rather different interpretation to the changes in the film over this potential region, based on cyclic voltammetry of polycrystalline foils in H_2SO_4. In their interpretation place exchange, i.e. surface phase oxide or hydroxide formation, becomes important already at 0.97V. With hydroxyl groups already established below the surface, the doubling of charge over the potential range 1.0-1.2V was ascribed to the oxidation of formal hydroxyl groups to formal oxygen atoms, i.e. a $1e^-$/Pt oxidative deprotonation leading to an anhydrous film which then becomes thicker at higher potentials. The major evidence cited for this was the invariance in the potential of the current maximum of the cathodic reduction curve, which suggested that there was no change in the Pt structure over this region. LEED has provided a more

direct indication of the extent of structural modifications at various potentials [29,31]. It suggests that the Pt-O structure is not invariant over the 1.0-1.2V range; rather, additional displacement of Pt atoms occurs towards 1.2V. In addition, the thermal desorption data argues against anhydrous films above 1.2V since the water desorption signal increased with the O_2 signal. While this water could be just adsorbed on top of an anhydrous layer, the similarity between the thermal water evolution peaks from the thin films and from the thick $Pt(OH)_4$ suggests that it is more likely water incorporated in a hydroxide. However, more conclusive determination of the nature of this water awaits the careful application of XPS and high resolution electron energy loss spectroscopy to these films.

The agreement of experimental TDS data with the perimeter-controlled desorption model indicates that thermal reduction occurs at the boundaries between covered and uncovered patches. Since thermal dehydration precedes thermal reduction, these conclusions pertain directly only to the anhydrous oxide layers derived from the anodic films. If the anodic film island geometry is not disturbed by dehydration the results also pertain to the anodic films themselves, and comparisons between thermal and electrochemical reduction can be drawn. In agreement with the proposed mechanism of thermal reduction, electrochemical reduction along patch edges has been proposed by Vetter and Schultze [5] for anodic films on Pt based upon the very small dependence of the Tafel slopes for cathodic stripping on film thickness. The implication of the perimeter desorption model that the film growth also proceeds though the reverse process of island growth and fusion at first seems counter to normal electrochemical thought, although at least one

investigation using three-parameter ellipsometry [8] has suggested the same result. Analysis of electrochemical charging curves has led to the conclusion that growth of anodic films proceeds by field-assisted place exchange between platinum atoms and oxygen from the electrolyte or oxide layer [5,48]. The basic experimental finding is that the anodic Tafel slope for a given film coverage or average thickness shows a linear dependence on the value of that film coverage. Following the Mott-Cabrera formalism [48], the rate of film growth is considered controlled by the potential gradient across the growing oxide layer, and the agreement of experimental data with the simple growth equation implies a uniform layer thickness. In other treatments [5] the important field gradient is considered to be that across the inner Helmholtz layer, and a uniform film thickness is not as directly implied. The apparent discrepancy between the island formation implied by TDS and high field growth indicated by electrochemical measurements is removed when it is remembered that electrochemical charging curves are sensitive only to the rate-limiting step in the initial oxidation of the surface, whereas the UHV transfer techniques, potentiostatic ellipsometry, and slow cathodic stripping measurements measure properties of the stable film produced at a given potential. Frequent reference has been made to aging processes in anodic films [5,7] whereby the initial oxidized surface rapidly rearranges to a more stable configuration. While initial oxidation may occur rather uniformly over the surface, as implied by the field-dependent place exchange model, the film rapidly rearranges to the island structure consistent with the TDS and stripping measurements.

The ability of the perimeter model to describe anodic film thermal desorption with a single activation energy from the lowest transferable

coverage up to saturation argues that, excluding the 10-15% multilayer contribution, a single chemical state exists on the surface for films formed by 2 min. anodization of Pt(100) at 1.2 to 2.2V. This observation agrees with some ellipsometric results in which constant optical properties were observed in this range [8,12], but disagrees with others [11]. The question as to whether the saturating and multilayer films are in the same oxidation state is less certain. The perimeter model shows the great extent to which film morphology can affect the kinetics of reduction. If thermal reduction of thin films occurs at contacts between oxidized and unoxidized patches, it seems reasonable that decomposition of multilayer films would occur only at higher temperatures where reduced sites could be nucleated throughout the phase. Thus the distinction between the 725K O_2 desorption peak and the O_2 desorbing at lower temperatures may very well be entirely due to film morphology and need not imply the presence of two chemically different compounds in the films. Although the similarity of water desorption for thick and thin films and the continuity of O_2 TDS behavior suggest that the thin as well as thick films have the composition $Pt(OH)_4$, unambiguous identification of the thin film composition will require techniques such as ESCA which were not available for cleanly transferred thin films in the present work. In the past, compounds in the Pt(+IV) oxidation state have been rejected as thin anodic film materials in part because the density (anodic charge/volume) of PtO_2 is too large to be consistent with both coulometry and measurements of thickness based on ellipsometry [12] or integrated ESCA peak measurements [13]. The present work indicates that the films formed at 1.2-2.2V are hydrated, probably in the form of a hydroxide.

No reliable crystal structures, or even density measurements, are available for Pt hydroxides, but they would be expected to have lower densities than the oxides of comparable metal oxidation state. For comparison, the crystalline density ratio for $Ni(OH)_2$:/NiO is 0.6 [49]. Assuming a $Pt(OH)_4$ composition and an approximate density, the thickness of the uniform part of the saturated thin film can be estimated. Thermal desorption of the saturated layer gave 2.3 O atoms desorbing as O_2 per Pt atom in the original surface, with ca. 15% of that in the multilayer desorption peak. The corrected 2.0 O/Pt corresponds to 2.6×10^{15} O cm^{-2}. Since $Pt(OH)_4$ decomposes with the overall stoichiometry

$$Pt(OH)_4 \text{ -----> } Pt + O_2 + 2\ H_2O$$

there is one $Pt(OH)_4$ unit per 2 oxygen atoms desorbing as O_2 or 1.3×10^{15} $Pt(OH)_4/cm^2$. If the density of $Pt(OH)_4$ is estimated as 0.6 times that of PtO_2, or $6g/cm_3$, then the uniform thickness of the saturated film is calculated to be 8Å. This estimated thickness is consistent with thickness measurements on polycrystalline Pt based on ellipsometry or ESCA, though it should be noted that both of these techniques would provide some form of a weighted average of the uniform and multilayer components of the film. The isotropic layer thickness for $Pt(OH)_4$, calculated as the cube root of the volume per formula unit, is 4Å, suggesting that the saturated uniform film on Pt(100) is an amorphous bilayer of $Pt(OH)_4$, with thicker patches containing 10-15% of the charge.

4.3 Thick layer formation

During rapid AC cycling between 0.5 and 2.2V the saturated thin layer with its small multilayer component is repeatedly formed. The lower potential limit is sufficient to reduce most of the saturated layer, but the small multilayer component, being more resistant to electrochemical, as well as thermal, reduction [47], is never reduced. After thousands of cycles the multilayer component accumulates, and a thick AC hydroxide is produced. The reason for the formation of the small multilayer component in the thin saturated film remains unclear. It may be related to statistical variations in local field strengths accompanying island formation during the aging of anodic films. Alternately, it may depend upon substrate defect concentrations. The latter possibility could be checked by the controlled introduction of bulk or surface defects to single crystal electrodes.

4.4. Comparison of TDS results with gas-phase data

4.4.1. Water TDS

Water desorbed from both thick and thin anodized films at temperatures 185K higher than those reported for the water-producing decomposition of surface-adsorbed hydroxyl layers produce by sequential dosing with oxygen and water in UHV [1]. The amount of water evolved from the thick films precludes its presence only at the surface of an anhydrous oxide; a hydrated

phase must be present. ESCA results suggested that this phase was a hydroxide rather than a hydrated oxide in which water retained molecular properties. The determination of the type of water in the thin anodic films is less certain, but the presence of the single water desorption peak identical in temperature and shape to that seen for the thick film suggests that here, too, the water was bound in the hydroxyl form. The difference in temperature from the gas phase results arises from the development of a phase hydroxide on the anodized surfaces as opposed to a surface adsorbed species. In the anodized films Pt atoms are displaced from their metallic positions [29] and are at least partially oxidized, and water can be strongly bound within the phase. Formation of the surface adsorbed hydroxyl species by gas-phase dosing does not disrupt the Pt lattice or significantly oxidize the surface Pt atoms, and water is less strongly bound.

4.4.2. O_2 thermal desorption

O_2 thermal desorption data for thin anodic films, thick anodic films, and gas-phase dosed Pt(100)(from ref. 23) are shown together for comparison in Fig. 10. While water evolved from the anodic films at temperatures substantially above those reported for hydroxides formed from the gas phase [1], O_2 evolved at somewhat lower temperatures than those reported for most surfaces exposed to oxygen in UHV. All anodic oxygen evolved at temperatures far lower than the 1200K ascribed by Salmeron et al. [25] to a surface phase oxide or oxygen in the near-surface region. No very broad bulk diffusion-limited O_2 desorption peaks such as might be expected for

subsurface [25] or dermasorbed [4] oxygen were observed, indicating that all oxygen resided at or very near the surface. Since all water desorbed at temperatures far below those required for the evolution of oxygen, the O_2 thermal desorption peaks for the anodic films correspond to the decomposition of an anhydrous surface phase oxide, and comparison with the anhydrous oxidized surfaces grown by gas-phase dosing is warranted.

Section 3.4.2 showed that the sharp peak shifting from 570 to 630K with increasing coverage and its shoulder at 640K could be described by a model in which desorption occurred at the perimeters of covered patches with the full thickness of the saturated layer, described in section 4.2 as a bilayer of $Pt(OH)_4$. In addition to these bilayer patches, about 15% of the anodic charge went into a TDS O_2 peak at 725K, ascribed to patches of multilayer $Pt(OH)_4$. It is impossible for all the O atoms desorbing from the saturated layer as O_2 and H_2O to fit into a single adsorbed atomic layer; the anodic films are clearly surface phases in which Pt-O place exchange has occurred. The gas phase data from ref. 23 shown in Fig. 10 are for a surface-adsorbed oxygen with an O/Pt surface atomic ratio of 0.6-1. The lower desorption temperatures observed for the surface phase oxides derived from the anodic films as compared to those for the gas phase dosed surfaces are probably due to this distinction between place-exchanged and surface-adsorbed layers.

Detailed comparison of the O_2 desorption data for thin anodic films with those for gas-phase dosed surfaces is complicated by disagreements between different sets of gas-phase results. Barteau et al. [24] found two desorption peaks on oxygen-dosed Pt(100), a low-coverage peak at 710K and an exceedingly sharp peak at 670K which grew in at higher coverages. The temperature of the high-temperature peak did not shift with coverage. The

coverage dependence of the sharp peak is not clear from the published data; however, the data were modeled with a first order process with a linear increase in desorption activation energy with increasing initial coverage. As shown in Fig. 8c, such a model produces an increase in T_p with increasing initial coverage, so it seems most probable that the data in Ref. 24 showed such an effect. Thus Barteau et al.'s data show striking qualitative agreement with the present data for thin anodic films, but their peaks occurred at ca.50K higher temperatures than the anodic film results and showed a lesser dependence of T_p on initial coverage. The temperature discrepancy led to multiple recalibrations of the temperature scale in the present work; the discrepancy appears to be real, not an experimental artifact. One is then faced with the curious situation that two different forms of oxygen on Pt(100) show qualitatively similar unusual sharp-peaked desorption behavior with similar dependencies on relative coverages, but at different temperatures. The absolute coverage dependence of the O_2 TDS from anodic films and from gas-phase adsorption also differ in that the gas-phase films saturate at ca. 0.7 O/surface Pt (even for high-temperature dosing) while the anodic films saturate at 2.0 O/surface Pt. Desorption at the perimeters of saturated patches could explain the similar qualitative behavior of both types of films, with the discrepancies in temperature and absolute coverage being brought by the different types of saturated layers grown by electrochemical vs. low pressure gas phase growth conditions.

Derry and Ross [23] also observed two-peak desorption for O_2 on Pt(100), with a low coverage peak and a sharp high-coverage peak at 660K. The T_p for their low-coverage peak moved to lower temperature for higher

initial coverages, as did the sharp peak, but their peaks lay in the same temperature ranges as those reported by Barteau et al. [24]. Derry and Ross' angle-resolved photoemission data indicated that their oxygen resided at the surface, while LEED data for cycled surfaces [29] indicated Pt/O place exchange in the anodic films. Overall, O_2 thermal desorption results on Pt(100) shows that O_2 evolves at temperatures between 575 and 750K for both the surface-adsorbed species and the phase oxides, both surface and bulk. Within this temperature window, the actual forms of the desorption peaks appear to be governed by complex kinetic factors with both geometric and energetic effects playing important roles. The desorption previously reported at higher temperatures [25-27] lies entirely outside our experience with any type of Pt oxide, (either bulk or surface) formed by sequential electrochemical oxidation and thermal dehydration.

The use of any ex situ technique in studying electrochemically generated layers is always frought with concern as to whether the surface as studied is relevant to the original surface in its electrochemical environment. Emersion and evacuation should cause, if anything, a decrease in the hydration of anodic films examined ex situ relative to their state in situ. Some dehydration was in fact observed when high vacuum and high energy electron beams were combined for AES measurements. The extensive hydration of the thin and thick films measured here in a UHV environment suggests that the films were hydrated to at least as great an extent within the electrochemical cell. While extreme caution must always be used in interpreting results from ex situ spectroscopies, the present results and those of other groups doing transfer experiments indicate that UHV techniques can provide unique

insights into the properties of electrode surfaces. At the same time electrochemical techniques can produce for study on single crystal surfaces chemical species which are inaccessible via other methods.

5. Conclusions

Anodic films formed on Pt above 1.1V(RHE) survived emersion and evacuation in a hydrated state and could be studied with UHV surface analytical techniques. All transferable films were hydrated to the extent of ca. 1 water molecule per $2e^-$ of anodic charge, or 1 water per O atom desorbing as O_2. Combined TDS and Pt 4f ESCA results shows that thick films formed by AC cycling had the stoichiometry $PtO_2 \cdot 2H_2O$. The ESCA 1s emission suggested that only hydroxyl oxygen was present in the thick film, identifying its composition as $Pt(OH)_4$. Upon heating, the thick film dehydrated at 400K and evolved oxygen at 715K. The oxygen and water contents of thin films formed at constant potential increased with potential up to 1.9V, where saturation occurred for the short growth times examined here. The saturated film contained 2.3 O atoms desorbing as O_2 and ca. 2 water molecules per surface Pt. Water desorbed from thin films with the same temperature and peak shape as that observed for thick films, suggesting that these films may also be hydroxides, though further spectroscopic evidence is required. The saturated thin film is suggested to be an amorphous bilayer of $Pt(OH)_4$ with a small multilayer component. O_2 desorption from thin films displayed complex kinetics which could be described by a model in which desorption occurs at the boundary between covered and uncovered portion of the surface. This

island-edge model is in agreement with previous studies of the kinetics of electrochemical reduction of anodic films on Pt [5]. The TDS results also suggest that the stable films emersed from electrolytes have an island structure, though the electrochemical rate-limiting step during anodic film growth may be the generation of a uniform layer which then reconstructs into islands. 10-15% of the O_2 from thin films desorbed in a peak around 725K, near that seen for thick films, indicating a small multilayer component in the thin films. No evidence was seen for significant dissolution of oxygen into bulk Pt on the timescale of these experiments.

Comparison of the unusual peak shapes of the present anodic film TDS results with previous studies of gas-phase dosed oxygen on Pt(100) suggests that desorption at the edges of saturated patches may control the kinetics in both cases, while the different temperatures and absolute coverages observed are due to the chemical differences between the two saturated layers, one place-exchanged and one surface-adsorbed. Oxygen is less strongly bound in the surface phase oxide derived from thin anodic films (ca. 20kcal/mol) than in gas-phase adsorbed layers (27-47kcal/mol [23,24]). On the other hand, water is much more strongly bound within the anodic films than in adsorbed hydroxyl layers formed by low-temperature coadsorption of oxygen and water vapor from the gas phase.

Acknowledgement

This work was supported by the Assistant Secretary for Conservation and Renewable Energy, Office of Advanced conservation Technology, Division of Electrochemical Systems Resources of the U.S. Department of Energy under Contract Number DE-AC03-76SF00098.

APPENDIX

In what follows are the details of two other models for the thermal reduction of Pt anodic films. These two models have some features in qualitative agreement with the observed TDS curves, but, for reasons discussed below, did not appear to be adequate physical models for the thermal reduction process.

Explicit autocatalytic desorption model

Oxygen TDS from anodic films was characterized by uncommonly sharp peaks. Similarly sharp peaks have been reported for the decomposition of formic acid on Ni(110) [50] and for O_2 desorption from Pt(100) [24]; in both cases the process was described as "autocatalytic." To test the relevance of the autocatalysis concept to the present data, two other models were examined, each also giving the requisite effective negative order of desorption. The first explicitly autocatalytic model assumes positive-order dependence on both covered and uncovered site concentrations, with the rate given by the equation

$$-d\theta/dt=\nu\theta^{m}(1-\theta)^{n}\exp(-E_a/RT).$$

The best match with data for peak sharpness and separation at different coverages (shown in Fig. 8b) was found for m=1 and 1<n<2, which produced the effective negative dependence on θ required by the data. The physical meaning of the 1<n<2 open site dependence and the very low preexponential factor

($5x10^6 s^{-1}$) is unclear. Baetzold and Somorjai [51] have shown that the rate equation for a desorption process limited by surface diffusion to active sites contains a preexponential factor which varies as the 3/2 power of the concentration of active sites. If a fixed fraction of sites (say a particular king configuration) were active when uncovered, and if the diffusion of oxygen to these sites were rate limiting, the 3/2 power dependence on $(1-\theta)$ and the low pre-exponential could be explained. The first-order dependence on θ would seem to require that all surface oxygen be mobile at the desorption temperature. This implied mobility seems inconsistent with the surface phase structure of the anodic film, in which O/Pt surface atomic ratios up to 2 are observed and in which Pt/O place exchange has occurred. This model, even when optimized, produced peaks for very high coverages which were more strongly separated from those for intermediate coverages than indicated by experiment. The model also does not predict the double-peaked structure seen in TDS, which must be assumed to be caused by a separate state or another decomposition pathway. While the explicit autocatalytic model can produce a sharp peak which shifts to higher temperature with coverage, it requires a series of restrictive and somewhat dubious assumptions to give a fit with data which is still inferior to that produced by the perimeter desorption model.

Variable activation energy desorption model

The second "autocatalytic" model tested, based on a model proposed by Barteau et al. [24] for O_2 adsorbed onto Pt(100) from the gas phase,

assumed desorption first order in occupied sites only, but with an activation energy which increases linearly with increasing coverage, i.e.,

$$-d\theta/dt=\nu\theta \exp[-(E_a+(\Delta E_a.\theta))].$$

Again, the parameters were juggled to provide proper peak temperature, peak sharpness, and temperature separation between high and intermediate coverage peaks, with the best fit shown in Fig. 8c. An increase in the activation energy from 20 to 24kcal/mol as θ increased from 0 to 1 was sufficient to produce a shift in T_p with initial coverage which mimics the experimental behavior. The pre-exponential factor of $2x10^7 s^{-1}$ seems too low for any rate limiting process except surface diffusion to active sites with a very low constant concentration. If surface diffusion is rate limiting, the first-order dependence again requires uniform oxygen distribution over the surface (i.e. mobility), which seems a non-physical assumption for a phase oxide. This model also does not predict the broad low coverage peak on top of which the sharp peak grows. While the first obtained from the variable activation energy model is better than that obtained from the explicit autocatalytic model, it gives less complete agreement with the experimental data for anodic films than does the perimeter desorption model of Fig. 8a.

References

[1] G.B. Fisher and B.A. Sexton, Phys. Rev. Let., 44 (1980) 683.

[2] S. Gilman, in Electroanalytical Chemistry, Vol. 2, A.J. Bard, ed., Marcel Dekker, New York (1967) p.111-192.

[3] T. Biegler and R. Woods, J. Electroanal. Chem., 20 (1969) 73.

[4] R. Thacker and J.P. Hoare, J. Electroanal. Chem., 30 (1971) 1.

[5] K.J. Vetter and J.W. Schultze, J. Electroanal. Chem., 34 (1972) 131, 141.

[6] M. Fleischmann, J.R. Mansfield, and Lord Wynne-Jones, J. Electroanal. Chem., 10 (1965) 511.

[7] H. Angerstein-Kozlowska, B.E. Conway, and W.B.A. Sharp, J. Electroanal. Chem., 43, (1973) 9.

[8] J. Horkans, B.D. Cahan, and E. Yeager, Surf. Sci., 46 (1971) 46.

[9] K.N. Reddy, M.A. Genshaw, and J.O'M. Bockris, J. Chem. Phys. 48 (1968) 671.

[10] S.H. Kim, W.K. Paik, and J.O'M. Bockris, Surf. Sci. 33 (1972) 617.

[11] J.L. Ord and F.C. Ho, J. Electrochem. Soc., 118 (1971) 46.

[12] R. Parsons and W.H.M. Visscher, J. Electroanal. Chem., 36 (1972) 329.

[13] J.S. Hammond and N. Winograd, J. Electroanal. Chem., 78 (1977) 55.

[14] O. Muller and R. Roy, J. Less Common Metals, 16 (1968) 129.

[15] M. Hecq and A. Hecq, J. Less-Common Metals 56 (1971) 133.

[16] E.S. Brandt, Ph.D. thesis, U. North Carolina, Chapel Hill,

[17] J.W. Schultze, Ber. Bunsenges. Phys. Chem., 73 (1969) 483.

[18] G.B. Fisher and J.L. Gland, Surf. Sci., 94 (1980) 435.

[19] B.A. Sexton, Surf. Sci., 94 (1980) 435.

[20] H. Ibach and S. Lehwald, Surf. Sci., 91 (1980) 187.

[21] J.L. Gland, Surf. Sci., 93 (1980) 487.

[22] C.T. Campbell, G. Ertl, H. Kuipers, and J. Segner, Surf. Sci., 107 (1981) 220.

[23] G.N. Derry and P.N. Ross, Jr., Surf. Sci. 140. 000 (1984).

[24] M.A. Barteau, E.I. Ko, and R.J. Madix, Surf. Sci., 102 (1981) 99.

[25] M. Salmeron, L. Brewer, and G.A. Somorjai, Surf. Sci. 112, (1981) 207.

[26] J.L. Gland, B.A. Sexton, and G.B. Fisher, Surf. Sci., 95 (1980) 587.

[27] B. Lang, P. Legare, and G. Maire, Surf. Sci., 47 (1975) 89.

[28] H. Niehus and G. Comsa, Surf. Sci. 102 (1981) L14.

[29] F.T. Wagner and P.N. Ross,Jr., to be published.

[30] F.T. Wagner and P.N. Ross,Jr., J. Electroanal. Chem., 150 (1983) 141.

[31] P.N. Ross, Jr. and F.T. Wagner, in Advances in Electrochemistry and Electrochemical Engineering, Vol. 13, H. Gerischer and C. Tobias, eds., J. Wiley and Sons, New York, 1984.

[32] F.T. Wagner and P.N. Ross, Jr., J. Electrochem. Soc., 130 (1983) 1789.

[33] P. Feulner and D. Menzel, J. Vac. Sci. Technol., 17 (1980) 662.

[34] J.A. Davies and P.R. Norton, Nucl. Instr. Meth., 168 (1980) 662.

[35] Varian Associates, Inc. Publ. No. 87-400 257

[36] J.L. Gland and V.N. Korchak, Surf. Sci., 75 (1978) 733.

[37] J.J. Randall, Jr., W.J. Bernard, and R.R. Wilkinson, Electrochim. Acta, 10 (1965) 183

[38] J.C. Huang, W.E. O'Grady, and E. Yeager, J. Electrochem. Soc., 125 (1977) 1732.

[39] G.A. Garwood and A.T. Hubbard, Surf. Sci., 112 (1981) 281.

[40] P.A. Redhead, Vacuum, 12 (1962) 203.

[41] N.R. Avery, J. Vac. Sci. Technol., 20 (1982) 592.

[42] D.A. King, in Chemistry and Physics of Solid Surfaces, Vol. 2, R. Vanselow, ed., CRC Press, Boca Raton, FL (1979) p. 87.

[43] J.R. Arthur and A.Y. Cho, Surf. Sci. 36 (1973) 394, J.R. Arthur, Surf. Sci. 38 (1973) 394.

[44] J.S. Mayell and S.H. Langer, J. Electrochem. Soc. 111 (1964) 348.

[45] S. Shibata, J. Electroanal. Chem., 89 (1978) 37.

[46] J. Balej and O. Spalek, Collect. Czech. Chem. Commun., 37 (1972) 499.

[47] J.D. Burke and M.B.C. Roche, J. Electroanal. Chem., 137 (1982) 175.

[48] A. Ward, A. Damjanovic, E. Gray, and M. O'Jea, J. Electrochemical Soc. 123 (1976) 1599.

[49] R.W.G. Wyckoff, The Structure of Crystals, The Chemical Catalog Company, NY, 1931.

[50] J.G. McCarty, J.L. Falconer, and R.J. Madix, J. Catal. 30 (1973) 235.

[51] R.C. Baetzold and G.A. Somorjai, J. Catal., 45 (1976) 94.

Figure captions:

Fig. 1. Unnormalized Auger spectra of Pt (100) after various stages of the transfer process.

Fig. 2. Oxygen/platinum auger peak ratio as a function of anodization potential.

Fig. 3. Integrated O_2 thermal desorption signal as a function of anodization potential. Signals were normalized to the overlap of the electrolyte contact area and the quadrupole nozzle aperture, then compared to the desorption signal for a saturation coverage of CO to allow O/Pt surface atomic ratios to be calculated (see text). O/Pt=1 corresponds to $2e^-$/Pt of anodic charge.

Fig. 4. Integrated H_2O thermal desorption signal as a function of electrode potential. Absolute coverage determined as in Fig. 3. Triangle gives datum for a surface exposed to rastered Auger beam.

Fig. 5. Auger spectrum for anodic film formed at 1.9V (RHE) on Pt (100) in 0.3M HF.

Fig. 6. O_2 and H_2O thermal desorption spectra for anodic film formed on Pt (100) at 1.8V (RHE).

Fig. 7. O_2 thermal desorption spectra for films formed at different potentials.

Fig. 8a. Perimeter desorption model. E_a = 21 kcal/mol, ν/d = $10^{14} cm^{-1} s^{-1}$. θ_o = 0.99, 0.85, 0.75, 0.60, 0.50, 0.38, 0.21.

Fig. 8b. Explicit autocatalytic model (see Appendix): E_a = 21 kcal/mol, m = 3/2, n = 1, $\nu = 5 \times 10^6$. θ_o = 0.99, 0.85, 0.75, 0.60, 0.50, 0.38, 0.21.

Fig. 8c. Linear increase in Ea with coverage (see Appendix): E_a = 20 kcal/mol, ΔE_a = 4, $\nu = 2x10^7$. θ_o = 0.99, 0.85, 0.75, 0.60, 0.50, 0.38, 0.21.

Fig. 9. O_2 and H_2O thermal decomposition spectra for a thick film formed by AC anodization of polycrystalline Pt foil. $dT/dt = 19Ks^{-1}$.

Fig. 10. Comparison of O_2 thermal desorption from: a,b,c, thin anodic films on Pt(100); d, thick anodic film; e, O_2 adsorbed from the gas phase on Pt(100) (ref. 21).

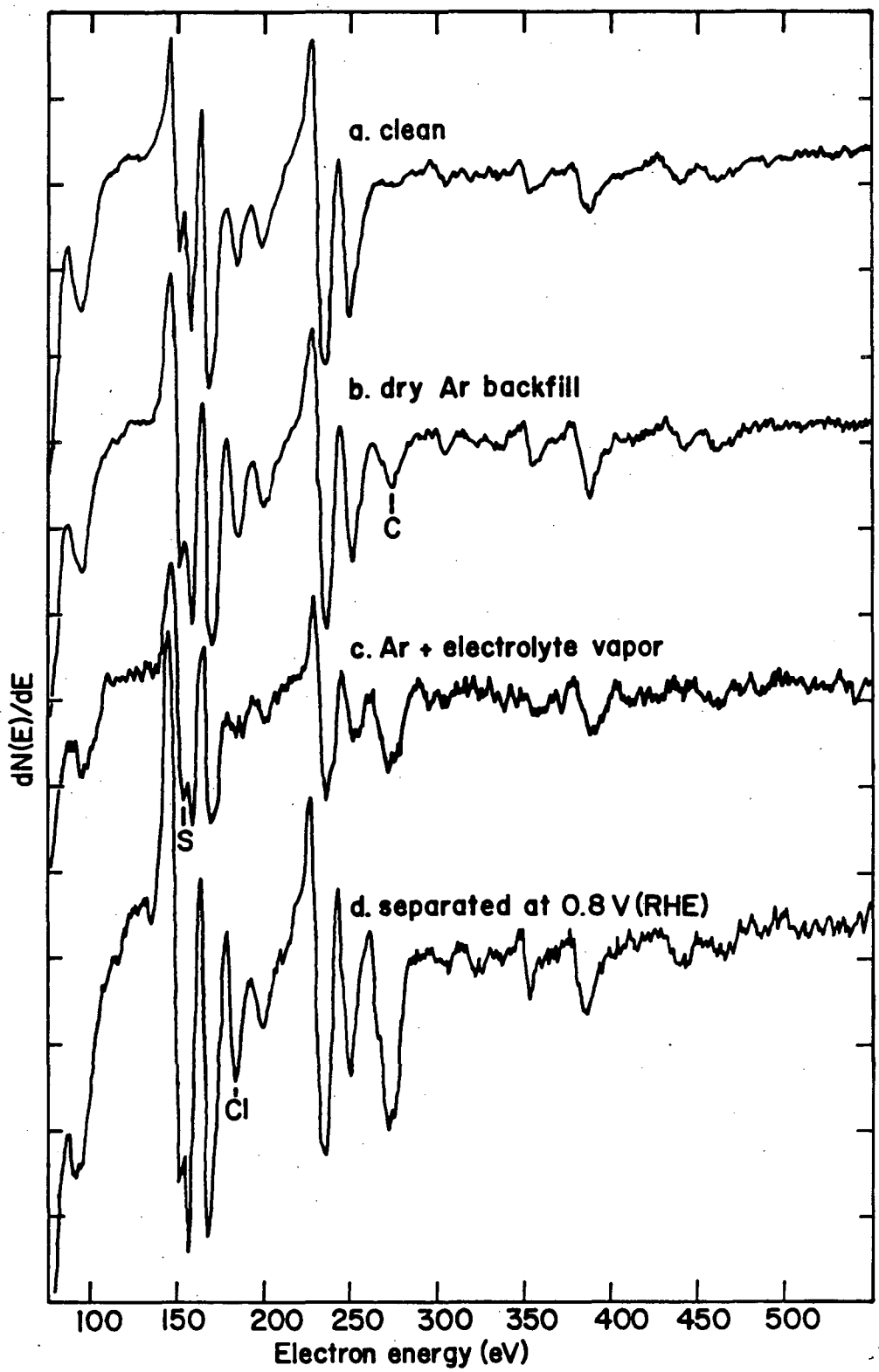

XBL 832-8234

Fig. 1.

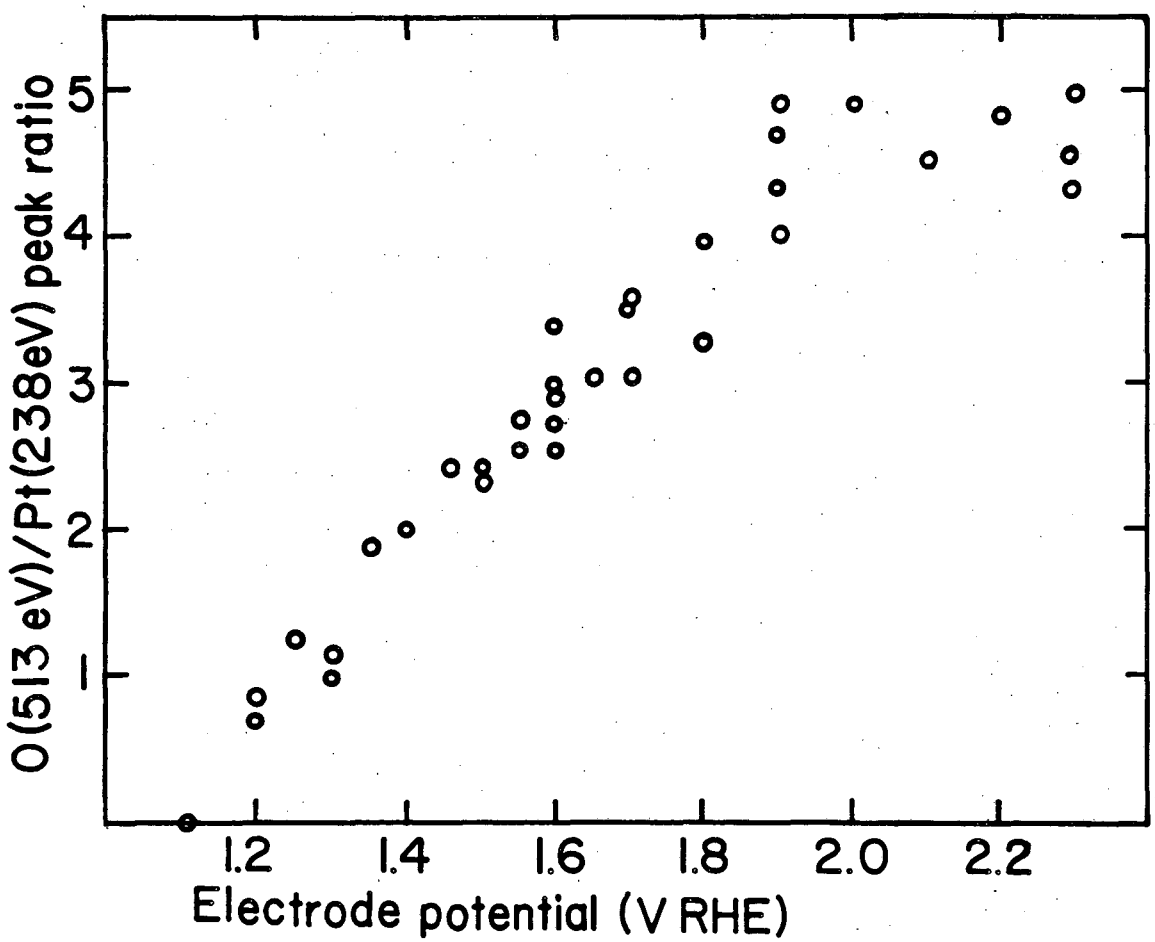

XBL 832-8435A

Fig. 2

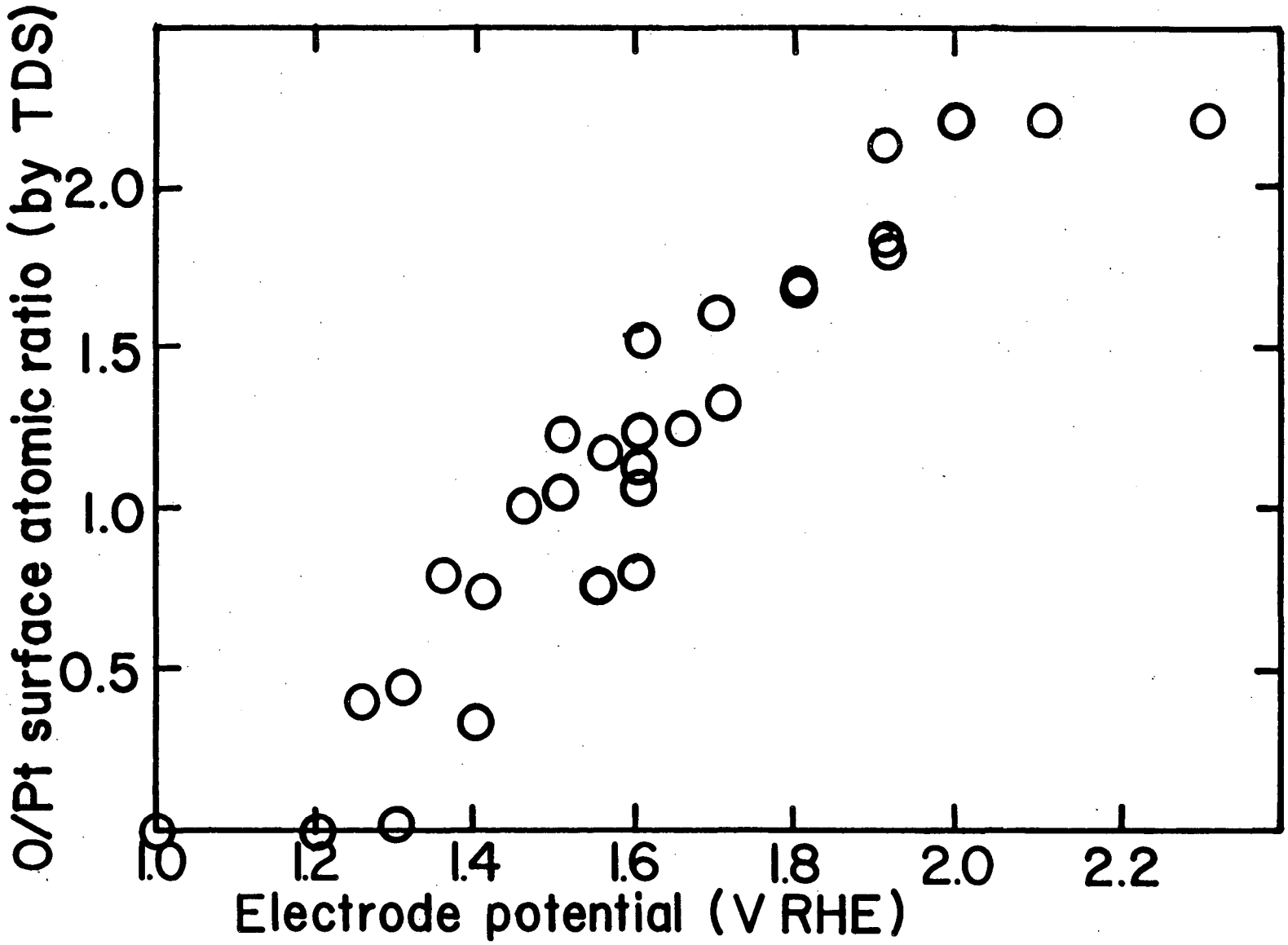

XBL 832-8428

Fig. 3

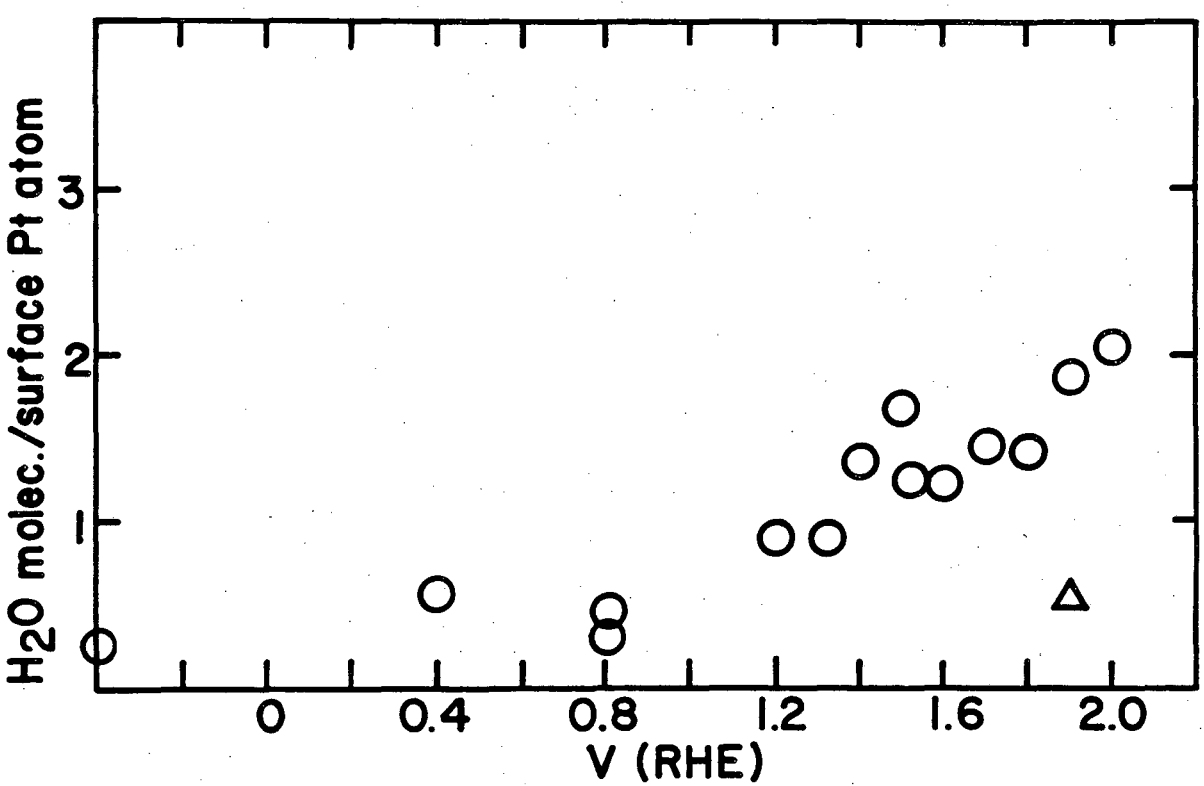

XBL 832-8433A

Fig. 4

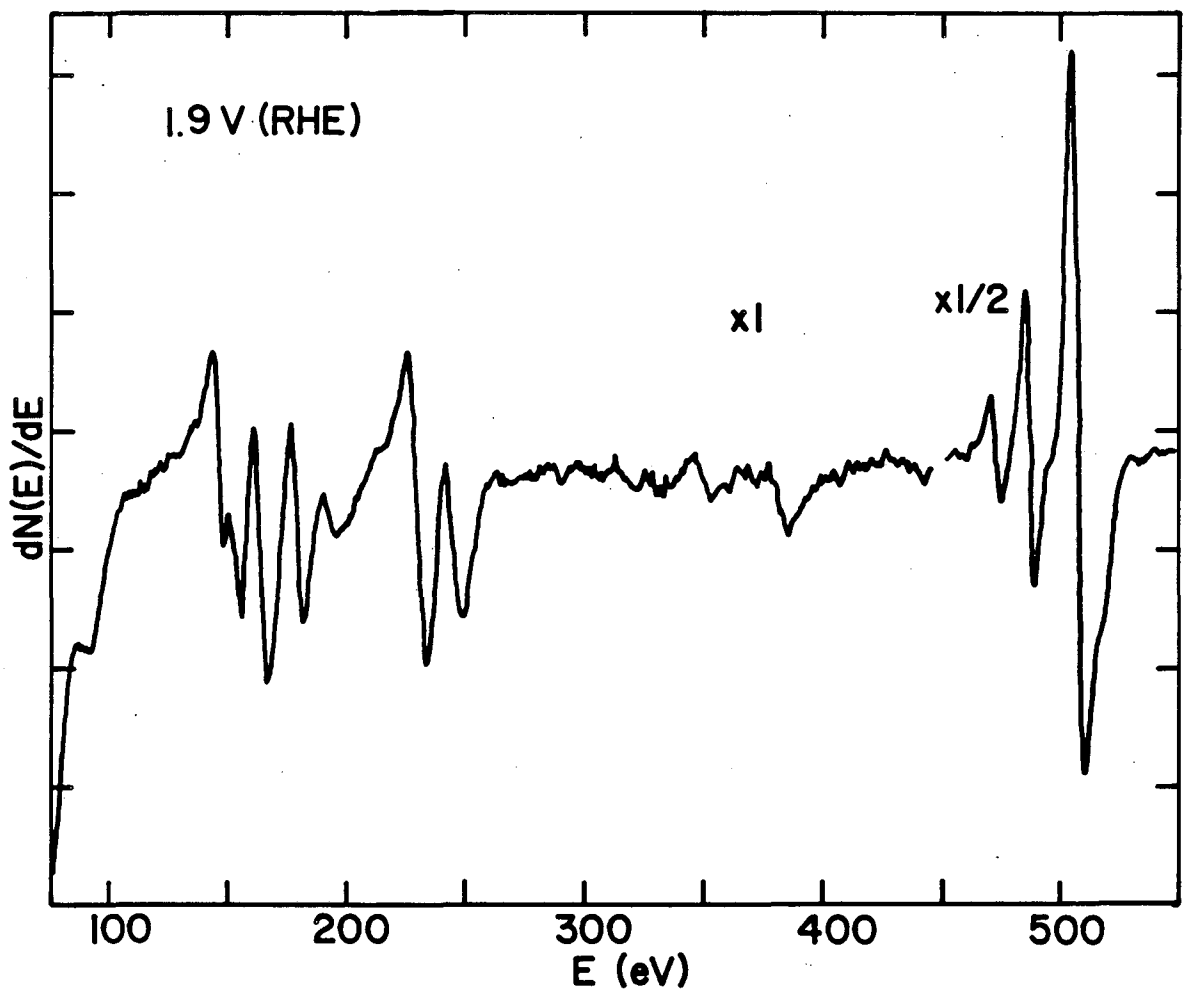

XBL 832-8439

Fig. 5

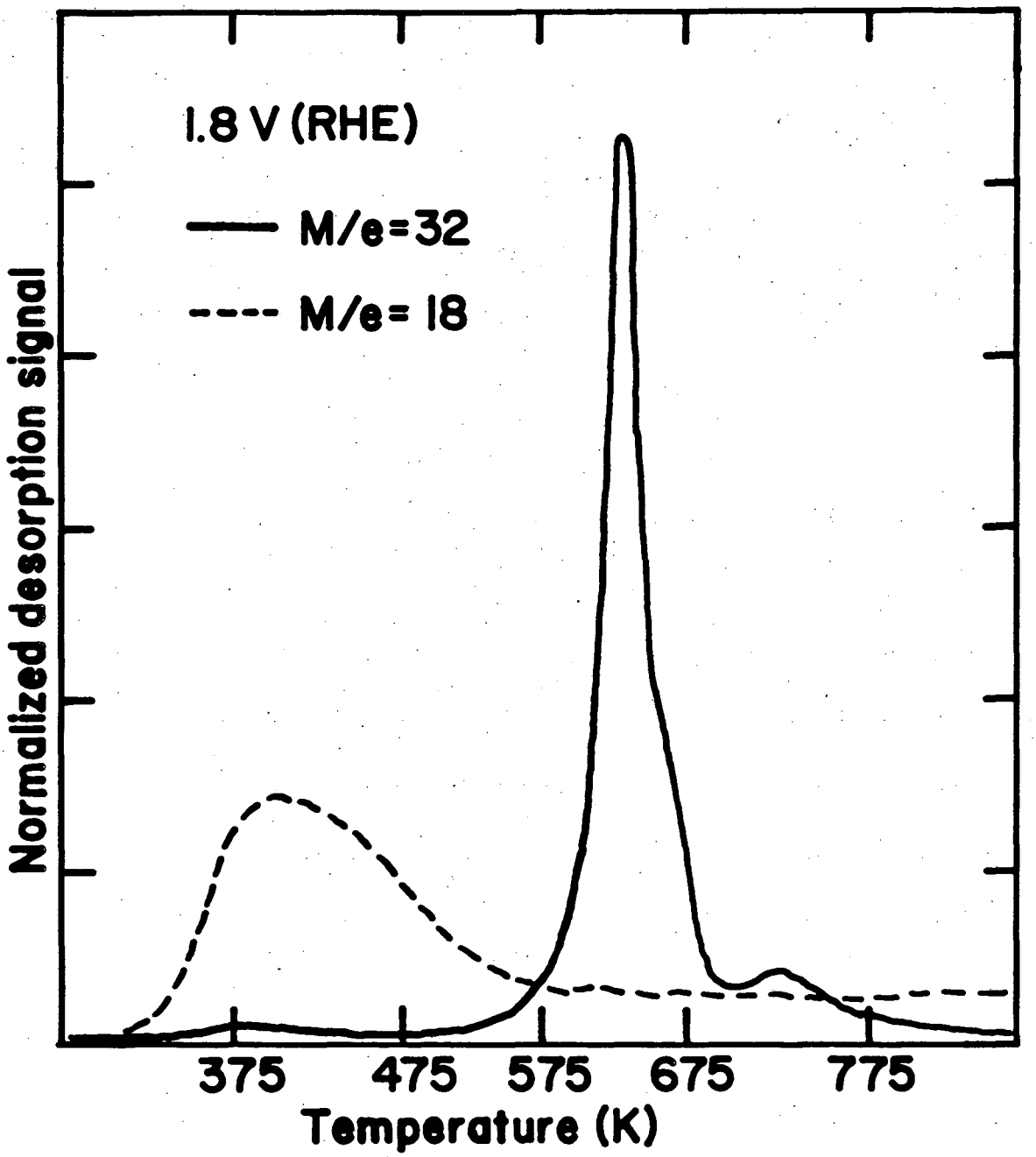

XBL 832-8429

Fig. 6

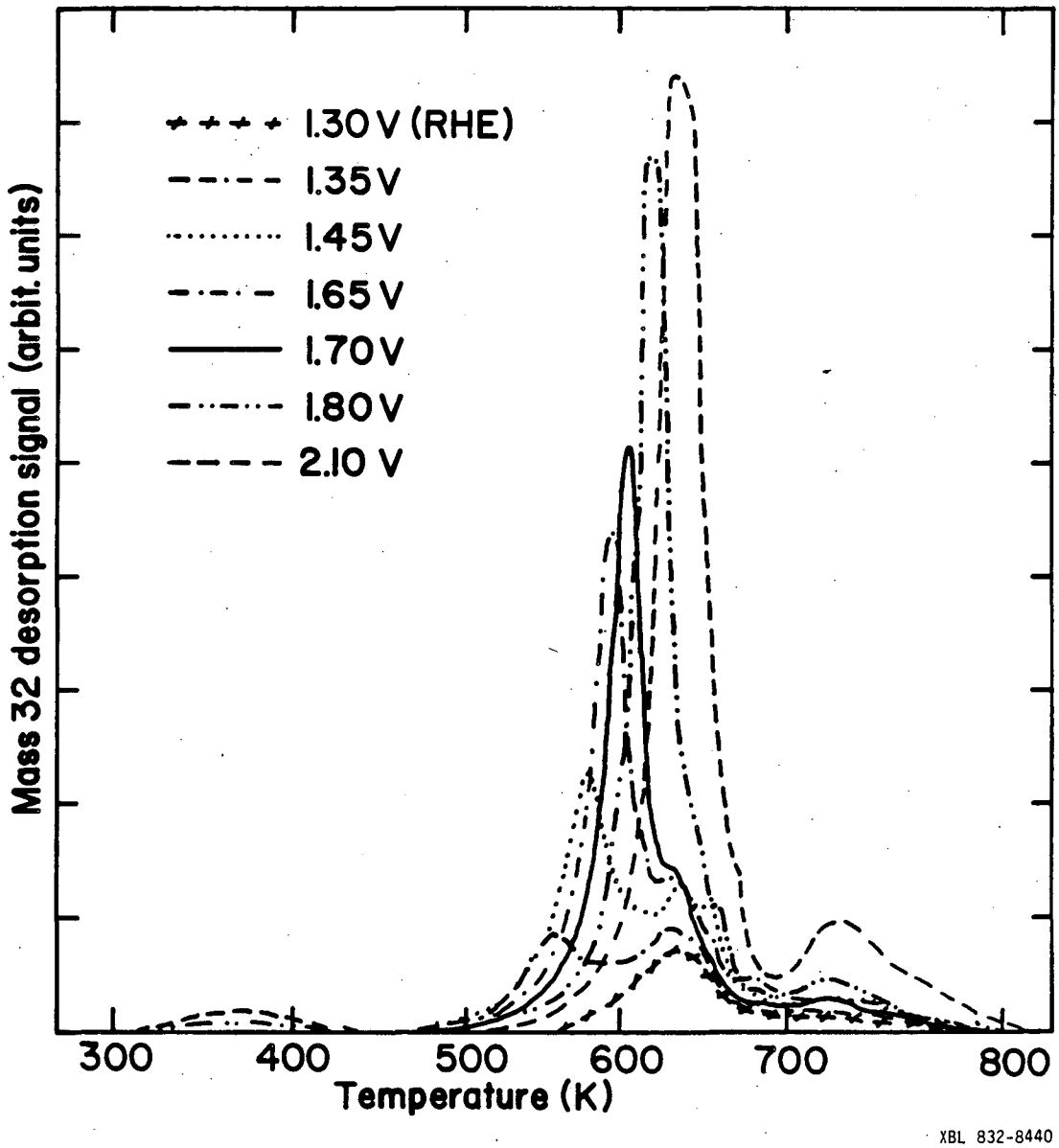
1.30 V (RHE)
1.35 V
1.45 V
1.65 V
1.70 V
1.80 V
2.10 V
Mass 32 desorption signal (arbit. units)
300
400
500
600
700
800
Temperature (K)
XBL 832-8440

Fig. 7

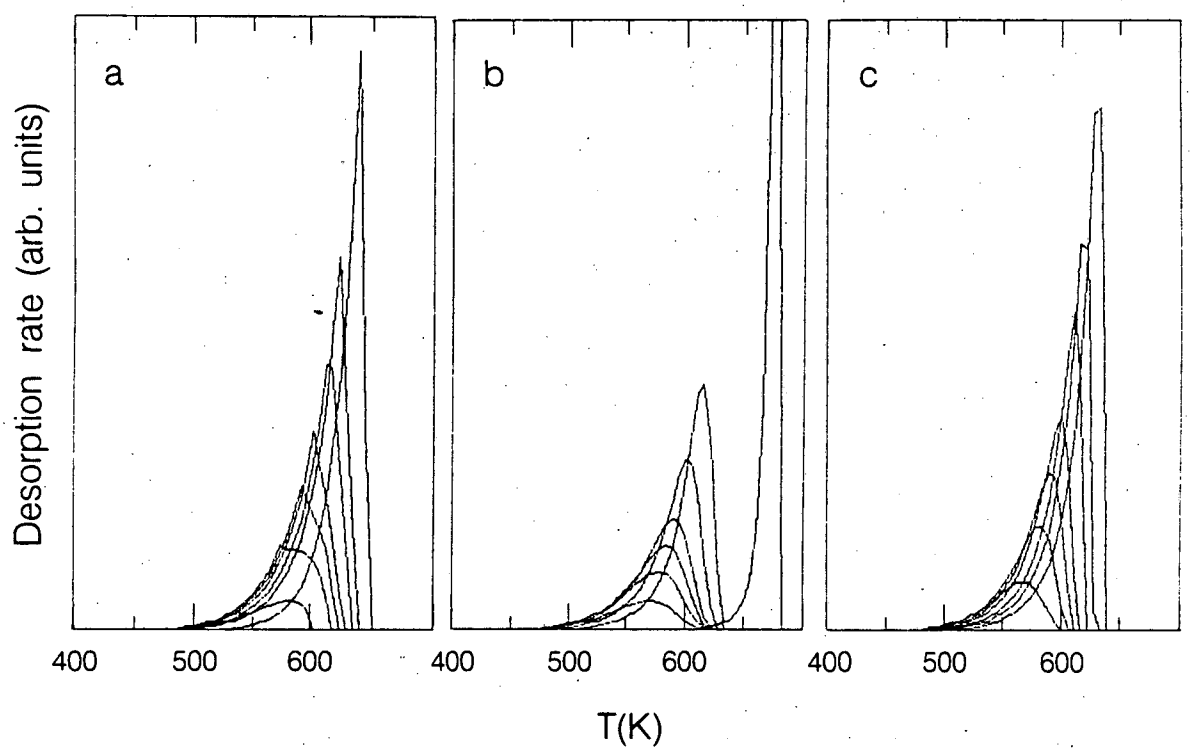

XBL 846-8967

Fig. 8

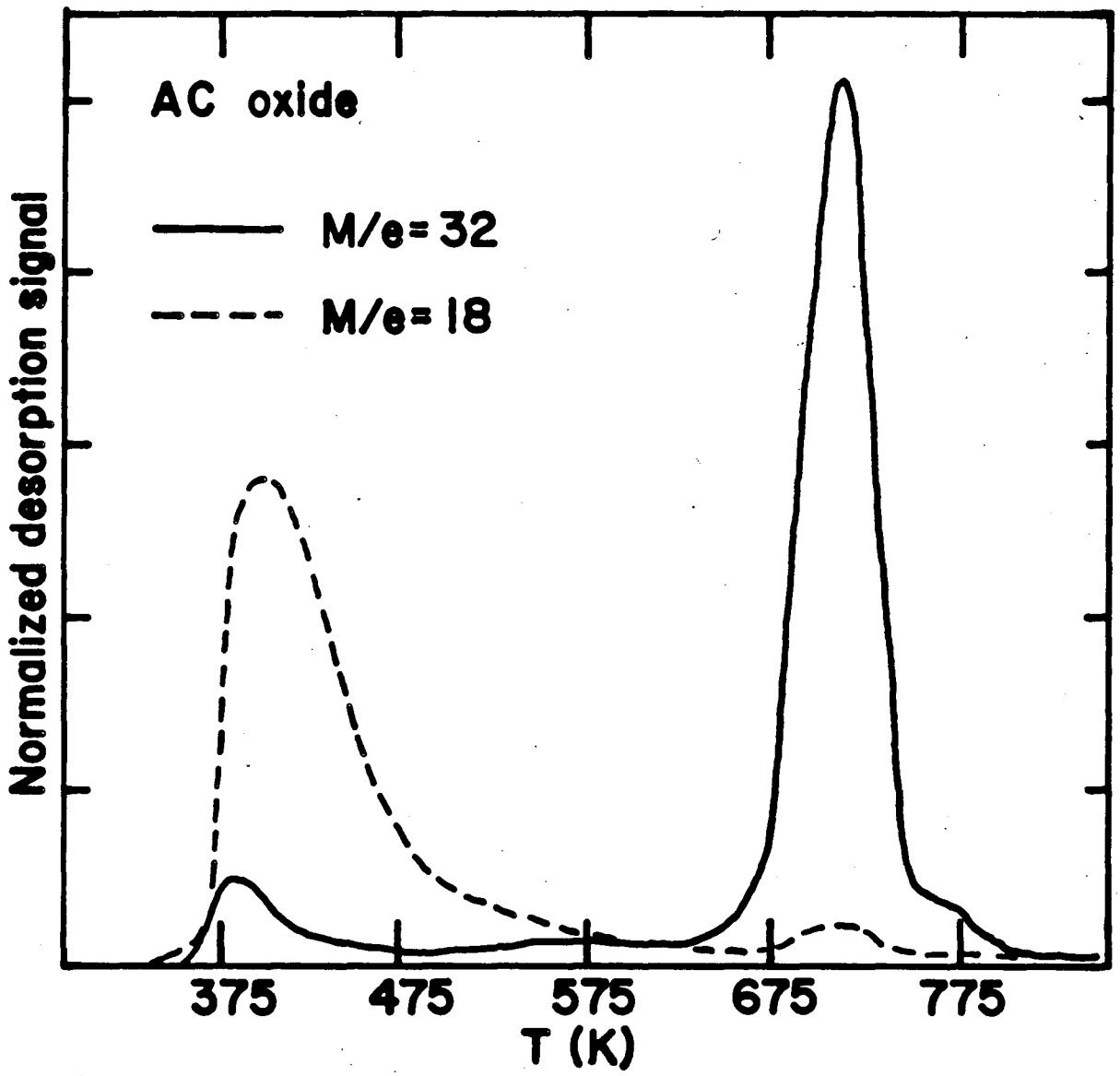

XBL 832-8430

Fig. 9

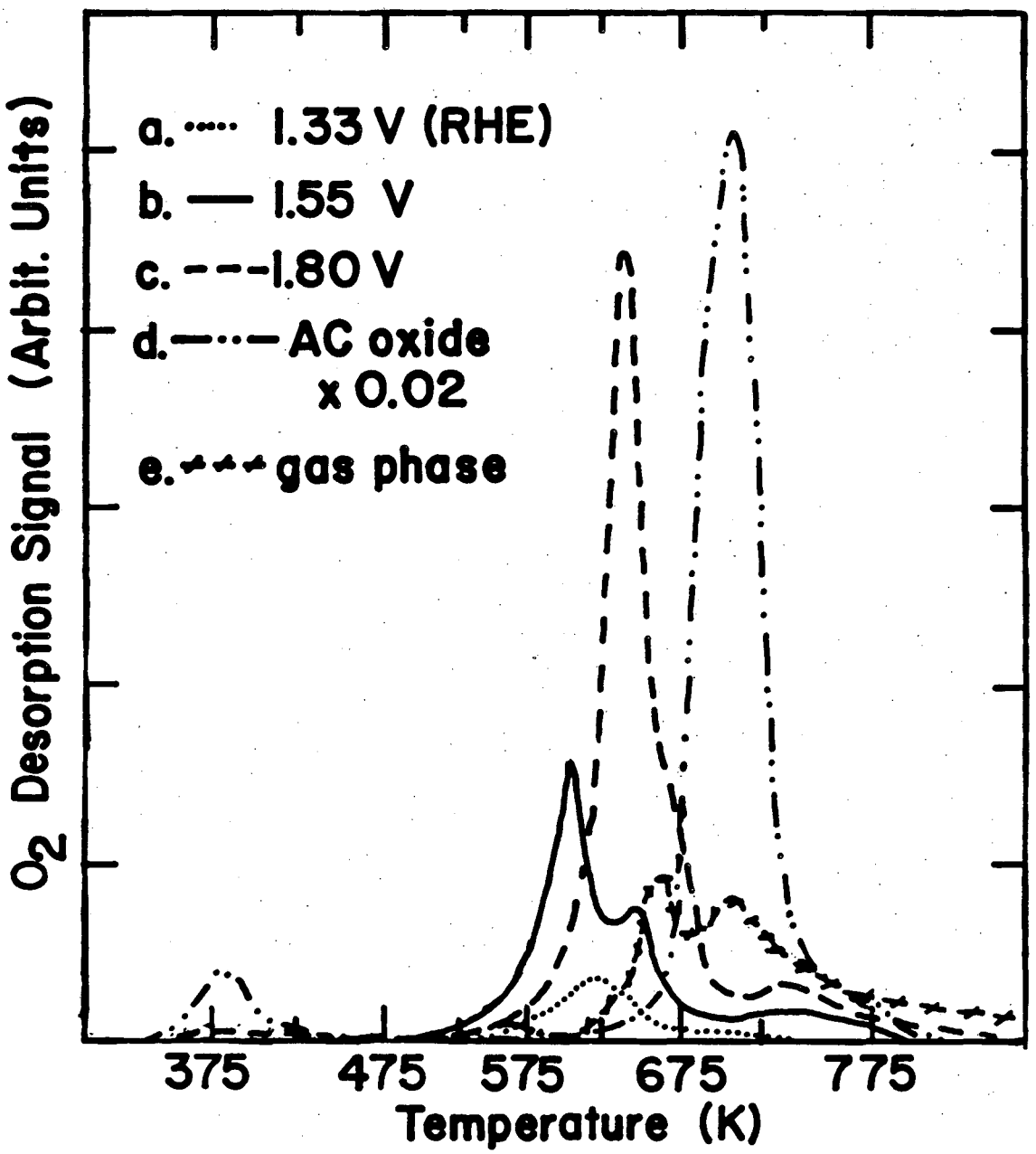

XBL 832-8437

Fig. 10

This report was done with support from the Department of Energy. Any conclusions or opinions expressed in this report represent solely those of the author(s) and not necessarily those of The Regents of the University of California, the Lawrence Berkeley Laboratory or the Department of Energy.

Reference to a company or product name does not imply approval or recommendation of the product by the University of California or the U.S. Department of Energy to the exclusion of others that may be suitable.

TECHNICAL INFORMATION DEPARTMENT
LAWRENCE BERKELEY LABORATORY
UNIVERSITY OF CALIFORNIA
BERKELEY, CALIFORNIA 94720